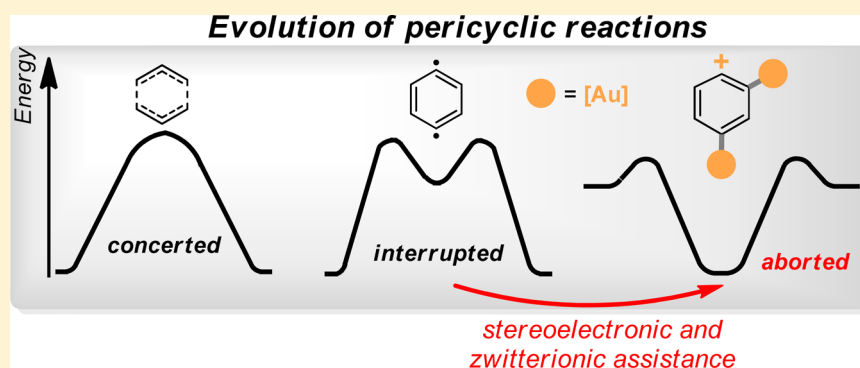


# Drawing Catalytic Power from Charge Separation: Stereoelectronic and Zwitterionic Assistance in the Au(I)-Catalyzed Bergman Cyclization

Gabriel dos Passos Gomes<sup>1b</sup> and Igor V. Alabugin\*<sup>1b</sup>

Department of Chemistry and Biochemistry, Florida State University, Tallahassee, Florida 32306-439, United States

**S** Supporting Information



**ABSTRACT:** The synergy between bond formation and bond breaking that is typical for pericyclic reactions is lost in their mechanistic cousins, cycloaromatization reactions. In these reactions, exemplified by the Bergman cyclization (BC), two bonds are sacrificed to form a single bond, and the reaction progress is interrupted at the stage of a cyclic diradical intermediate. The catalytic power of Au(I) in BC stems from a combination of two sources: stereoelectronic assistance of C–C bond formation (i.e., “LUMO umpolung”) and crossover from a diradical to a zwitterionic mechanism that takes advantage of the catalyst’s dual ability to stabilize both negative and positive charges. Not only does the synergy between the bond-forming and charge-delocalizing interactions lead to a dramatic (>hundred-billion-fold) acceleration, but the evolution of the two effects results in continuous reinforcement of the substrate/catalyst interaction along the cyclization path. This cooperativity converts the BC into the first example of an aborted [3,3] sigmatropic shift where the pericyclic “transition state” becomes the most stable species on the reaction hypersurface. Aborting the pericyclic path facilitates trapping of cyclic intermediate by a variety of further reactions and provides a foundation for the discovery of new modes of reactivity of polyunsaturated substrates. The application of distortion/interaction analysis allows us to quantify the increased affinity of Au-catalysts to the Bergman cyclization transition state as one of the key components of the large catalytic effect.

## INTRODUCTION

Out of the three main approaches to the formation of cyclic structures (i.e., cyclizations,<sup>1</sup> pericyclic reactions,<sup>2</sup> and cycloaromatizations<sup>3</sup>), cycloaromatization reactions are by far the most unusual and difficult to control.<sup>4</sup> Whereas the number of bonds (paired electron pairs) is generally conserved in cyclizations and pericyclic reactions, the number of broken bonds is not equal to the number of formed bonds in cycloaromatization reactions. Instead, in cycloaromatizations, two unstable reactive centers (e.g., two radicals) are created from a closed-shell molecule where all electrons are paired. In contrast, a typical cyclization reaction generally involves a “preformed” high energy reactive center (e.g., a cation, a radical, or an anion) that attacks a weak functionality (e.g., a  $\pi$ -bond) in a process where one bond is formed and the other is broken. Common pericyclic processes such as cycloadditions or ring closures proceed through a mechanism where the “first-order changes in bonding”<sup>5</sup> are concerted, so the number of broken

bonds and the number of formed bonds are again the same (Figure 1).

The cycloaromatization reactions form a cycle by trading two  $\pi$ -bonds for a single  $\sigma$ -bond in a process that involves an asynchronous evolution of the two seemingly disconnected orthogonal  $\pi$ -systems into diradicaloid intermediates.<sup>6</sup> The in-plane  $\pi$ -orbitals are transformed into the new bonds and the two nonbonding orbitals (e.g., two radicals) on the route through the transition state (TS) to the product, whereas the out-of-plane  $\pi$ -orbitals provide a stabilizing effect at the post-TS stage by forming an aromatic system. The generation of two reactive centers from a closed-shell precursor accounts for the unique advantages of these processes in organic synthesis,<sup>7</sup> drug design,<sup>8</sup> polymer, and materials science.<sup>9</sup>

Received: October 23, 2016

Published: February 10, 2017

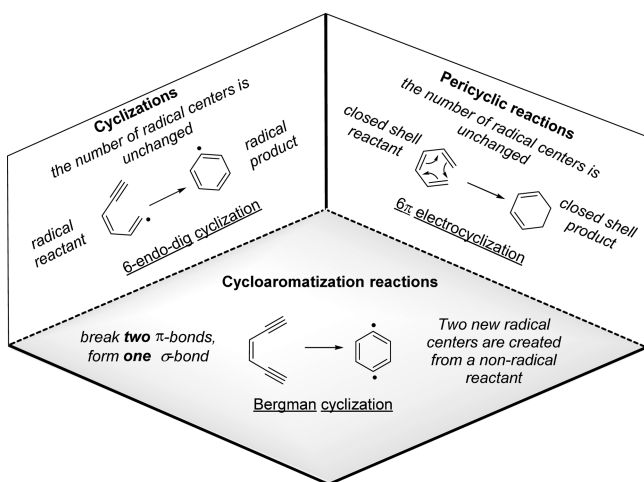
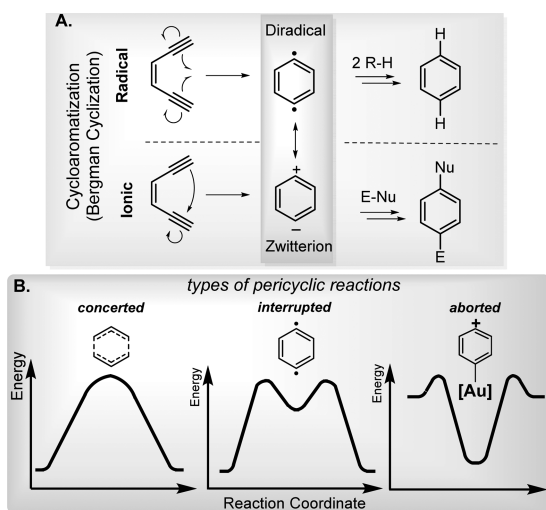


**Figure 1.** Comparison of radical cyclizations and electrocyclic ring closures with cycloaromatization reactions. Note that the total number of out-of-plane  $\pi$ -bonds changes in pericyclic reactions but not in cycloaromatization reactions and radical cyclizations.

The parent cycloaromatization process, the Bergman cyclization,<sup>10</sup> involves an interesting and complex combination of electronic changes that render this process a fertile testbed for the development of new theoretical methods. This deceptively simple transformation of enediyne leads to *p*-benzynes,<sup>11</sup> a chemical chameleon with reactivity ranging between the diradical and zwitterionic extremes (Scheme 1).<sup>12</sup>

**Scheme 1.** (A) Diradical/Zwitterionic Dichotomy in Cycloaromatization of Enediyne (Note That Two Zwitterionic Structures Are Possible for Nonsymmetric Molecules); and (B) Three Types of Pericyclic Reactions

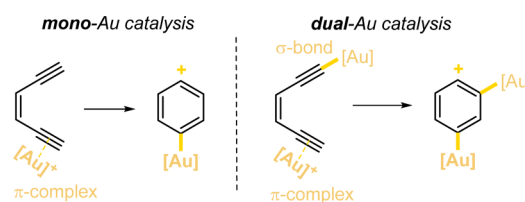


Although discovered only recently,<sup>13</sup> the dichotomy between the radical and zwitterionic reactivity of *p*-benzynes is a manifestation of one of the most general dilemmas of chemistry. Every time a chemical bond is broken, there is the choice between nonpolar and polar extremes. Not surprisingly, it hides under the surface of other cycloaromatization processes and, more generally, reactions where bond formation and bond cleavage are not synchronized.<sup>14</sup>

The recent explosion of Au-catalyzed cycloaromatizations<sup>15–18</sup> is reflected in several reports of Au-catalyzed

Bergman cyclizations, some of them leading to ions trapped by nucleophiles.<sup>19</sup> Several features of these reactions are noteworthy: (a) they proceed at much lower temperatures than the parent BC, (b) they lead to polar intermediates, and (c)  $C_1$ – $C_5$  (Schreiner–Pascal) cyclization can be competitive with the  $C_1$ – $C_6$  (Bergman) at ambient conditions. Intriguingly, it was found that both  $C_1$ – $C_6$  and  $C_1$ – $C_5$  products can be formed through the same TS<sup>20</sup> and the ratio of these two products is determined by dynamic effects at post-transition state bifurcations.<sup>21</sup> However, most of these interesting observations were made under the “dual  $\sigma,\pi$ -catalysis”<sup>22</sup> conditions where two Au-species were coordinated to the enediyne moiety in  $\sigma$ - and  $\pi$ -fashions, respectively (Scheme 2).

**Scheme 2.** Comparison of Mono-Au(I) ( $\pi$ -type) Catalysis and “Dual  $\sigma,\pi$ -Catalysis”



There has been no theoretical analysis of the parent mono-Au(I) ( $\pi$ -type) catalysis mode in the Bergman cyclization. Not only is this parent process conceptually important, but it also provides the main Au-activation mechanism for enediyne with terminal substituents where the dual  $\sigma,\pi$ -catalysis is impossible. The goal of this work is to evaluate the magnitude of  $\pi$ -catalysis computationally, compare it with  $\sigma,\pi$ -catalysis, and create the theoretical framework for understanding the nature of catalytic effects in this class of reactions.

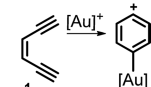
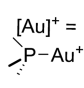
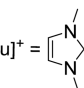
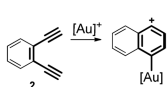
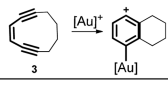
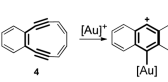
## RESULTS AND DISCUSSION

**Effect of Au-Coordination on the Potential Energy Surface for the Bergman Cyclization.** The calculated barriers and reaction energies for the representative set of substrates and catalysts are summarized in Table 1. Coordination of  $[\text{Me}_3\text{P-Au}]^+$  to one of the triple bonds has a dramatic effect on BC; the barrier is decreased from 31.8 to 16.1 kcal/mol, and the cyclization becomes  $\sim 6$  kcal/mol exergonic. Similar accelerating effects were found for the other enediyne substrates. For the parent reaction, we have also evaluated the effect of catalyst structure on reactivity. The effects are significant; more cationic Au species provide a greater decrease in the activation barrier.

Solvent effects on reactivity are shown in Table 2. In contrast to the noncatalyzed Bergman cyclization where effects of solvents are negligible, the Au-catalyzed process is sensitive to the solvent polarity. Two trends are observed. First, the binding energy between reactant and substrate decreased as the solvent polarity increased. On the other hand, the activation barriers became larger in the more polar solvents (15.4 in vacuum vs 16.5 kcal/mol in  $\text{CH}_3\text{CN}$ ). The latter trend suggests that transition state/catalyst is less polar than the reactant/catalyst complex, in agreement with the increased charge transfer from the substrate to the cationic Au-species in the TS.

**Electronic Structure Analysis.** Why is the Au-catalyzed BC TS much earlier and lower in energy in comparison to its noncatalyzed counterpart? What are the reasons for these pronounced differences? The first part of the puzzle is revealed

Table 1. Computational Analysis of the Au-Catalyzed and Noncatalyzed BC for a Selection of Enediyne<sup>c</sup>

Reaction	$E_{comp}^a$	$\Delta E_{cat}^\ddagger$ <sup>b</sup>	$\Delta E_{rxn}^b$ <sup>b</sup>	$\Delta E_{rxn}^\ddagger$ <sup>b</sup> noncat
				
$[Au]^+ =$ 	-29.4 (-30.5)	<b>14.6</b> <b>(15.8)</b>	<b>-7.3</b> <b>(-1.7)</b>	
$[Au]^+ =$ 	-34.6	16.5	-6.3	31.0 (29.2)
$[Au]^+ =$ AuCl	-38.9	20.4	-0.5	
	-32.1	<b>13.7</b>	<b>-0.6</b>	31.9
	-37.0	<b>10.9</b>	<b>-6.1</b>	27.6
	-33.5	<b>6.1</b>	<b>-7.3</b>	21.6

<sup>a</sup>Relative to isolated reactant and catalyst. <sup>b</sup>Relative to reactant–catalyst complex. <sup>c</sup>(IEFPCM = toluene)/(U)PBE0/6-311+G(d,p)/Def2-TZVP+ECP level of theory. (SMD = toluene)/CCSD(T)/6-311++G(d,p)/Def2-TZVP+ECP single point corrections in parentheses. Energies in kcal/mol.  $[Au]^+ = [Me_3P-Au]^+$ , unless stated otherwise.

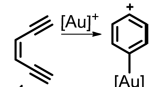
by the differences in the evolution of bond-forming  $\pi_{CC} \rightarrow \pi_{CC}^*$  interactions along the two reaction coordinates. For the Au-catalyzed BC, the bond-forming interactions start to increase in magnitude much earlier and grow much faster (Scheme 3).

We will show below that these differences come from two components: (a) a stereoelectronic reorganization, that is, “LUMO umpolung”,<sup>23</sup> and (b) the zwitterionic character of this reaction promoted by the ability of the Au-moiety to stabilize both the negative and the positive charges.

**Stereoelectronic Assistance.** For the noncatalyzed case, the magnitude of bond-forming two-electron  $\pi \rightarrow \pi^*$  interactions drops to zero when the two interacting orbitals approach an unproductive region (at the “Nicolaou’s threshold”, i.e.,  $C_1-C_6$  distance ca. 3.2 Å, Scheme 3). Because of the node present in the alkyne  $\pi^*$  orbital, bonding interactions between the enediyne  $C_1$  and  $C_6$  are mostly canceled by the antibonding interactions between  $C_2$  and  $C_5$  when at the parallel geometry that resembles the TS of symmetry-forbidden thermal  $[2_s+2_s]$  cycloaddition<sup>24</sup> (Scheme 3). The contribution of unfavorable  $\pi^*$ -symmetry diminishes slowly on the route to the TS where  $C_2-C_5$  distances become much larger than the  $C_1-C_6$  distance.

In contrast, the Au-catalyzed reaction is free of this stereoelectronic burden because of the change of the alkyne MO symmetry. This change is associated with a  $3c,2e$ -bond

Table 2. Computational Analysis of Solvent Effect in the Au-Catalyzed and Noncatalyzed BC for a Selection of Enediyne<sup>c</sup>

solvent	$E_{comp}^a$	$\Delta E_{cat}^\ddagger$ <sup>b</sup>	$\Delta E_{rxn}^b$ <sup>b</sup>	$\Delta E_{rxn}^\ddagger$ <sup>b</sup> noncat
				
No solvent ( <i>vacuum</i> )	-40.8	15.4	-8.0	31.0
toluene ( $\epsilon = 2.37$ )	-29.4	14.6	-7.3	31.0
THF ( $\epsilon = 7.43$ )	-24.6	15.9	-7.1	30.9
DCM ( $\epsilon = 8.93$ )	-24.1	16.0	-7.0	30.9
DCE ( $\epsilon = 10.12$ )	-23.9	16.1	-6.9	30.9
MeCN ( $\epsilon = 35.69$ )	-22.6	16.5	-6.4	30.9

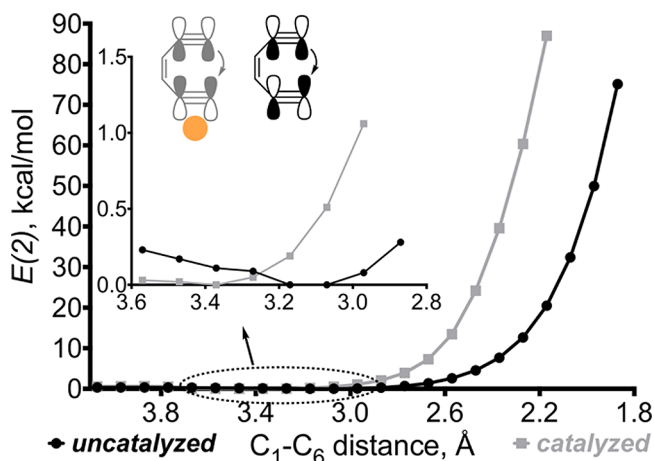
<sup>a</sup>Relative to isolated reactant and catalyst. <sup>b</sup>Relative to reactant–catalyst complex. <sup>c</sup>(IEFPCM = solvent)/(U)PBE0/6-311+G(d,p)/Def2-TZVP+ECP level of theory. Energies in kcal/mol.  $[Au]^+ = [Me_3P-Au]^+$ .

formation between an alkyne and an empty Au-orbital that translocates the  $\pi^*$ -node (Scheme 4B) away from the bond-forming region. We refer to this change in the symmetry of the antibonding orbital as “LUMO umpolung”,<sup>1,25</sup> because from the point of view of the reacting partner the LUMO of the alkyne-catalyst complex is analogous to the HOMO of the initial alkyne.

We have shown earlier that this symmetry change has important consequences in cyclization reactions<sup>25</sup> (Scheme 4A) where it provides a viable approach to the design of *endo*-selective cyclizations. Such cyclizations are stereoelectronically disfavored when nucleophile adds to a nonactivated  $\pi$ -bond. Nucleophile’s *endo*-attack at the alkyne LUMO leads to the Nu–C bond-forming two-electron interaction but is disfavored by the LUMO symmetry. On the other hand, the symmetry-allowed interaction of nucleophile with the alkyne HOMO involves fully occupied orbitals and hence cannot lead to bond formation.

Symmetry-allowed two-electron interactions can be activated by switching either to an electrophilic cyclization or to an electrophile-promoted nucleophilic cyclization (EPNC). In the latter scenario, the *endo*-cyclizations are facilitated when the attacked  $\pi$ -bond is pre-coordinated to an external Lewis acid (i.e., in the electrophile-promoted nucleophilic cyclizations or EPNCs). This change is due to the removal of destabilizing secondary orbital interaction associated with the node in the

Scheme 3. A Closer Look at the Evolution of  $\pi_{CC} \rightarrow \pi_{CC}^*$  Interactions throughout PES for Both Noncatalyzed and Catalyzed Bergman Cyclizations<sup>a</sup>



<sup>a</sup>“Nicolaou’s threshold” for Bergman cyclization corresponds to the region where the bond-forming interactions for the noncatalyzed process are symmetry-forbidden. For the Au-catalyzed process, bond formation is symmetry-allowed due to “LUMO umpolung” as shown in the inset (see Scheme 4 and in text for the discussion of “LUMO umpolung”). Only in-plane orbitals are shown for enediyne. The out-of-plane MOs are bystanders that do not directly participate in this reaction.  $E(2)$  stands for second-order interactions and are obtained via NBO analysis.

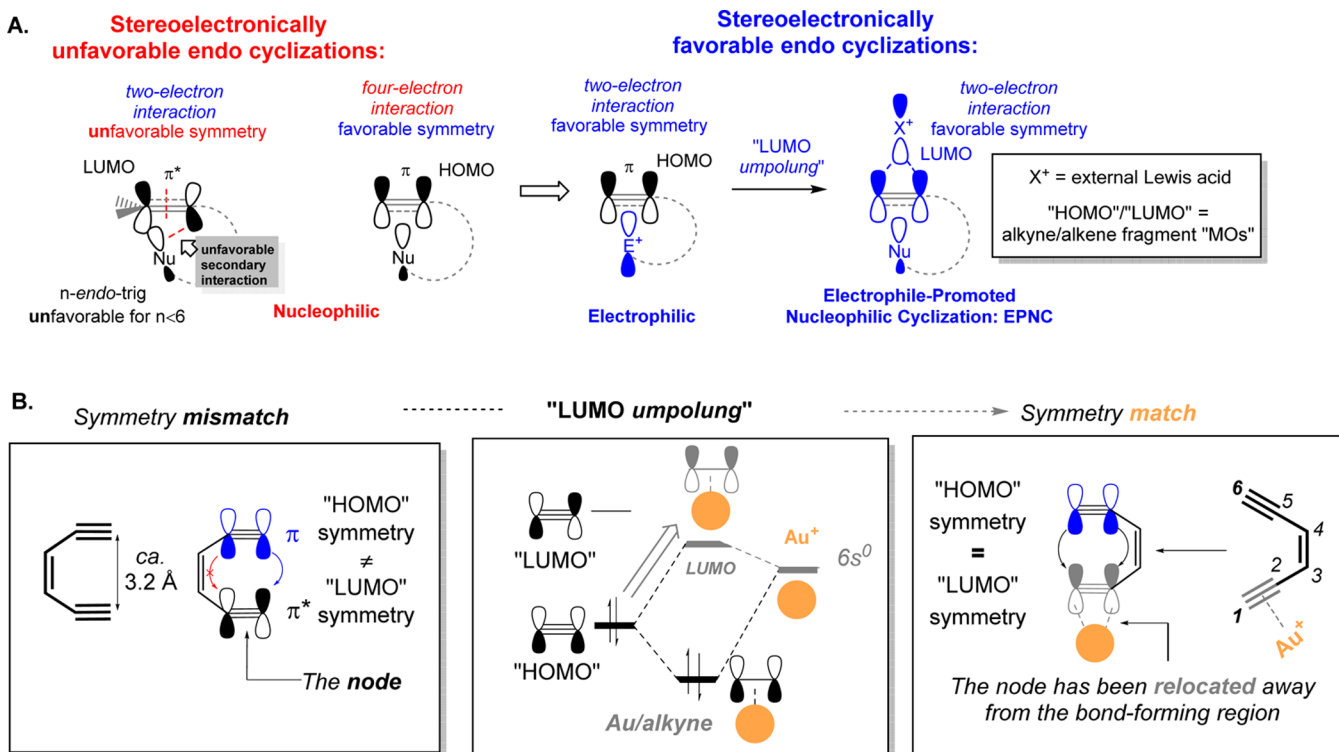
$\pi^*$ -orbital. In other words, there is no node between the two carbon atoms of the  $\pi$ -bond because the LUMO of the  $\pi$ -complex is created from the  $\pi$ -orbital (rather than  $\pi^*$ ). Because of this change of orbital symmetry, EPNCs stereoelectronically resemble electrophilic cyclization where the target  $\pi$ -bond (e.g., alkyne HOMO) is attacked by a cation in the cycle-closing step. However, unlike cationic cyclization, EPNCs of alkynes do not suffer from thermodynamic penalty of creating an sp-hybridized vinyl carbocation inside of a cyclic structure.

Scheme 4B illustrates how the concept of LUMO umpolung is expanded to cycloaromatizations. Unlike the “symmetry-forbidden” noncatalyzed process, the “[2+2]” interaction between the HOMO of alkyne and LUMO of alkyne/catalyst complex becomes symmetry-allowed due to the change in the alkyne LUMO symmetry caused by Au-coordination. Not only does the present work expand, for the first time, the utility of LUMO umpolung to cycloaromatizations, it also suggests that the concept of LUMO umpolung may be used for the design of thermal symmetry-allowed [2+2] cycloadditions.<sup>26</sup>

As a result of LUMO umpolung, the bond-forming  $\pi \rightarrow \pi^*$  interaction between the in-plane  $\pi$ -orbitals continuously increases along the Bergman cyclization path (Scheme 3). In summary, the stereoelectronic component to Au-catalysis is based on helping the  $\sigma_{CC}$  bond to form faster by making the interactions between the filled and vacant in-plane  $\pi$ -orbitals symmetry allowed. However, this is only one component of the catalytic effect.

**Zwitterionic Assistance.** Analysis provided in this section will show the second role of Au-coordination, its assistance in

Scheme 4. (A) Earlier Use of “LUMO Umpolung” for Solving Symmetry Mismatch for Nucleophilic Cyclizations<sup>1</sup> (“HOMO” and “LUMO” Correspond to Fragment Molecular Orbitals); and (B) Applying “LUMO Umpolung” toward Bergman Cyclization<sup>a</sup>

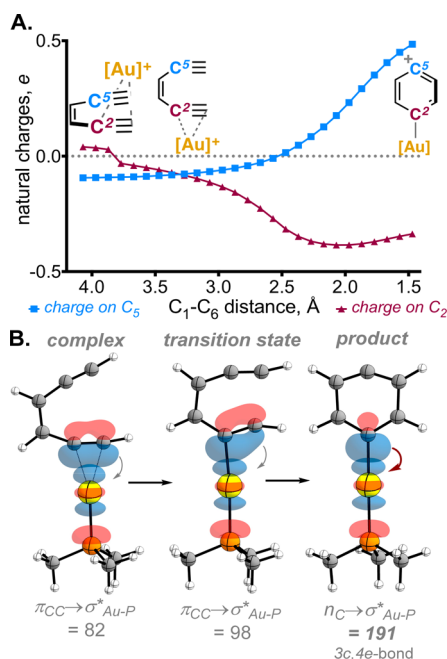




the development of latent zwitterionic reactivity usually hidden in thermal cycloaromatizations of hydrocarbons. We have suggested earlier that effects of metal coordination in cycloaromatization chemistry can lead to stabilization of both the cationic and the anionic species depending on the Au position in the products.<sup>12b</sup> In this work, we reveal full details of this assistance for the first time.

The charge separation in the Au-catalyzed BC continuously increases as this molecular system moves along the reaction path (Scheme 5). Its onset coincides with the beginning of C–

**Scheme 5.** (A) Evolution of Natural Charges at C<sub>2</sub> and C<sub>5</sub> throughout the Au-BC (Note Increase in Polarization along with Its Asynchronicity); and (B) Evolution of  $\pi_{CC} \rightarrow \sigma_{Au-P}^*$  Interactions<sup>a</sup>



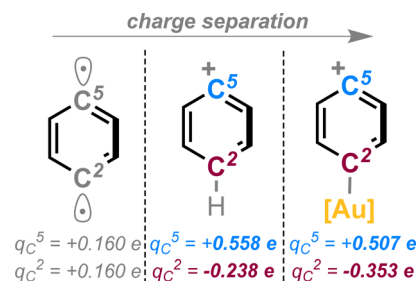
<sup>a</sup>Selected NBO interactions are in kcal/mol. As the alkyne moieties interact to form the new C–C bond, the  $\pi$ -complex becomes a C–Au  $\sigma$ -bond.

C bond formation, and its overall evolution provides insight into the electronic dynamics of this reaction. C<sub>5</sub> has its charge gradually increased as expected, because this atom will bear the positive center in the product. On the other hand, the charge on C<sub>2</sub> decreases until the end of the process, where seemingly unexpectedly it stops declining and even rises again.

**Charge Distribution.** In *p*-benzyne, the radical-bearing carbons C<sub>2</sub> and C<sub>5</sub> are essentially neutral (charge of +0.16 e). In contrast, the same carbons in the Au-catalyzed reaction have much larger and opposite charges of -0.35 e and +0.51 e, respectively. This charge separation is bigger than the analogous separation in the phenyl cation (Scheme 6).

**Stabilization of Negative Charge.** The asynchronicity of the above changes originates from charge transfer to the metal. This behavior displays the catalyst's higher affinity to the substrate in the transition state and product of this reaction (Scheme 5B). One piece of evidence for increased transfer of electron density to the catalyst is provided by Natural Bonding Orbital (NBO)<sup>27</sup> analysis that identifies very strong interactions between the substrate and the [Au] moiety. The donor orbital evolves from a  $\pi$ -bond in the reactant and TS to a lone pair at

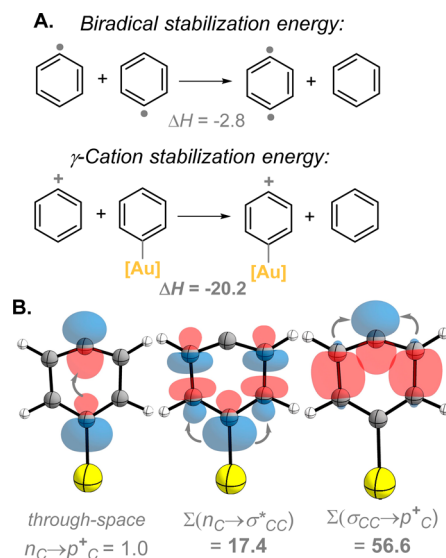
**Scheme 6.** Increase in Charge Separation Caused by the Presence of [Au]



C<sub>2</sub> in the product. As the reaction progresses, donation from these orbitals to the  $\sigma_{Au-P}^*$  orbital strongly increases. The NBO energies in Scheme 5 should be considered a crude estimate of such interactions because they are clearly too large to be treated by a second-order perturbative approach.<sup>27</sup>

**Stabilization of Positive Charge.** In addition to stabilizing the developing negative charge, the Au-moiety provides stabilization of the cationic center as well. This stabilization is evident from the two equations shown in Scheme 7A. The top one is the classic evaluation of through-

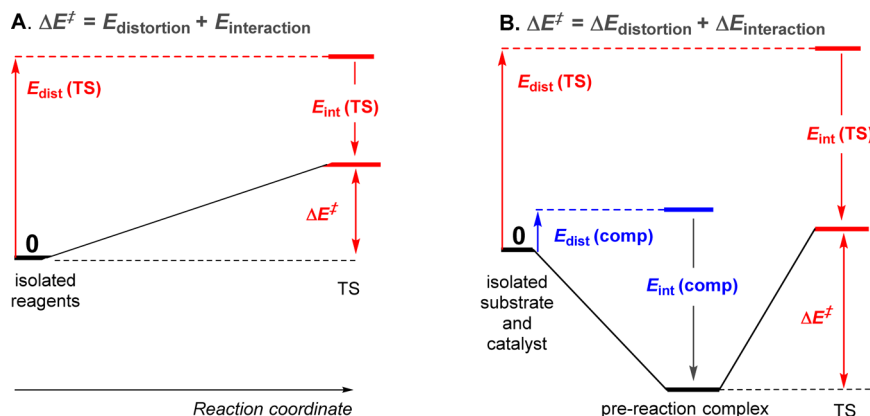
**Scheme 7.** (A) Top, Stabilization in *p*-Benzyne Stems from the through-Bond Coupling between the Two Radical Centers; Bottom, Stabilization in the Product of Au-Catalyzed BC Is Dramatically Larger than That Found in *p*-Benzyne (Energies in kcal/mol); and (B) Selected NBO Interactions (in kcal/mol) Stabilizing the Positive Charge in the Product<sup>a</sup>



<sup>a</sup>PR<sub>3</sub> group omitted for clarity.

bond (TB) coupling between the two radical centers via the biradical stabilization energy (BSE). This electronic effect provides ~3 kcal/mol of stabilization to *p*-benzyne and explains its significantly lower reactivity to H-donors when compared to phenyl radicals.<sup>28</sup> This orbital interaction was applied for the design of other radical reactions.<sup>29</sup> Remarkably, we find that the analogous estimate for the stabilizing effect of the para C–Au bond on the cationic centers is much larger (20 kcal/mol). This stabilization leads to delocalization of positive charge in the Au-Bergman product in comparison to the parent phenyl cation.

Scheme 8. Two Variations of Distortion-Interaction Analysis: (A) A Bimolecular Reaction Analyzed by Comparison of Isolated Reactants and the TS; and (B) “Unimolecular” Reaction Promoted by Coordination with a Catalyst and Analyzed via Comparison of the Prereaction Substrate/Catalyst Complex (“comp”) with the TS



Such interaction corresponds to the classic double hyper-conjugation pattern known to stabilize  $\delta$ -substituted cations.<sup>30</sup>

The combination of negative and positive charge delocalization accounts for the utility of Au-catalysis in bringing the latent zwitterionic nature of the Bergman cycloaromatization process to the surface. However, quantifying the relative contributions of the above effects is complicated by the multimode nature of Au–enediynes interactions and their complex evolution along the reaction path.

**Distortion-Interaction Analysis.** To quantify the stabilizing effect of Au/substrate interactions in this reaction, we suggest an alternative approach, the distortion–interaction analysis. The essence of this method is in comparing energies of the two isolated substrates with the energies of the interacting pairs at the key reaction geometries. Distortion describes the energy penalty for changing the ideal geometries of the separated reactants, whereas interaction energy reflects energy lowering due to covalent and noncovalent interaction between the reactants.

This approach was used for bimolecular reactions to compare two isolated reactants with their respective transition state.<sup>31</sup> The important conceptual distinction of our approach with the analysis of simple bimolecular cycloadditions is that we determine distortion and interaction energies for the catalyst and substrate in both the reactant and the transition states of a catalyzed “unimolecular” process. Such dissection of catalytic processes is useful because it allows one to distinguish unproductive reactant stabilization from productive TS stabilization. This is important because only TS stabilization leads to the catalytic effect on the reaction.

Not only does Scheme 8 illustrate this aspect, but it also clearly shows that the reaction barrier for the catalyzed “unimolecular” processes can be expressed in eq 1 that includes activation and distortion energies for the catalyst/substrate prereaction complex and for the activation complex:

$$\Delta E^\ddagger = (E_{\text{dist}}(\text{TS}) + E_{\text{int}}(\text{TS})) - (E_{\text{dist}}(\text{comp}) + E_{\text{int}}(\text{comp})) \quad (1)$$

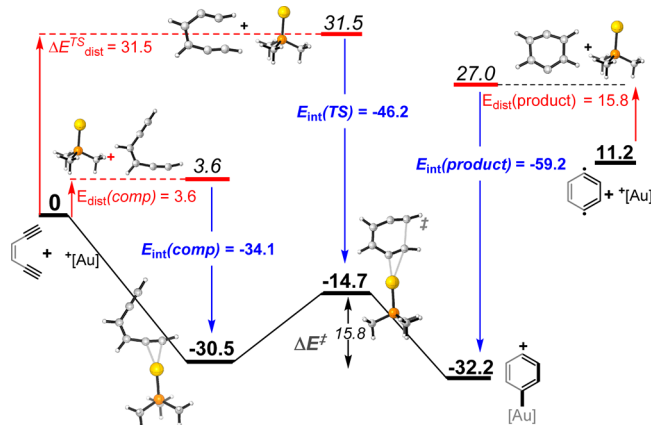
Furthermore, eq 1 can be also rewritten as eq 2 that expresses the barrier for a catalyzed reaction in terms of changes in the distortion and interaction energies upon transition of the substrate/catalyst complex to the activation complex. For the catalyst to be effective, it needs to either decrease the cost for

substrate distortion or increase its interaction energy with the substrate. Because the two effects can be either synergistic or anticooperative, it is helpful to use eq 2 to evaluate the interplay between these two components quantitatively.

$$\begin{aligned} \Delta E^\ddagger &= (E_{\text{dist}}(\text{TS}) - (E_{\text{dist}}(\text{comp}))) \\ &+ (E_{\text{int}}(\text{TS}) - E_{\text{int}}(\text{comp})) = \Delta E_{\text{dist}} + \Delta E_{\text{int}} \quad (2) \end{aligned}$$

This analysis (Scheme 9) reveals two stages in the Au-catalyzed Bergman cyclization. In the first of them, Au/

Scheme 9. Application of Distortion-Interaction Analysis to the Au-Catalyzed Bergman Cyclization<sup>a</sup>



<sup>a</sup>The right part of the scheme takes this analysis even further and applies it to the product by comparing it with the isolated *p*-benzynes and the Au-catalyst. Single-point energies, in kcal/mol, at the (SMD = toluene)/CCSD(T)/6-311++G(d,p)/Def2-TZVP+ECP level of theory.

enediynes coordination relocates the node for “LUMO umpolung” and prepares the productive orbitals for the bond-forming interaction. The large exergonicity of the Au/substrate complex formation stems from the large interaction energy (~34 kcal/mol) that can overcome a small distortion penalty (~4 kcal/mol). Such large reactant stabilization can be counterproductive unless compensated by an even greater transition state stabilization.

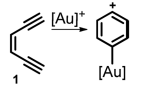
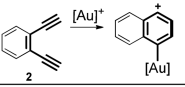
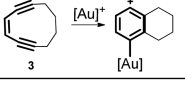
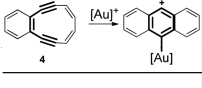
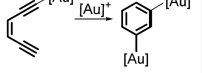
Analysis of the Au/TS coordination in Scheme 9 reveals that the TS is significantly more distorted from the ideal

Table 3. Computational Analysis of Three Au-Catalyzed Bergman Cyclizations of the Parent Enediyne<sup>c</sup>

Catalyst	$E_{dist}(comp)$	$E_{int}(comp)$	$E_{dist}(TS)$	$E_{int}(TS)$	$\Delta E_{int}^c$	$\Delta\Delta E^{\ddagger d}$
	4.5 (3.6)	-33.9 (-34.1)	34.0 (31.5)	-48.6 (-47.3)	-14.7 (-13.2)	16.4 (13.4)
	5.0	-39.6	34.3	-50.8	-11.2	14.5
AuCl	7.0	-45.9	34.9	-55.3	-9.4	10.6

<sup>a</sup>Relative to isolated reactant and catalyst. <sup>b</sup>Relative to reactant–catalyst complex. <sup>c</sup>Between TS and reactant complex (catalyzed reaction). <sup>d</sup>Barrier lowering relative to the noncatalyzed reaction. <sup>e</sup>Calculations at (IEFPCM = toluene)/(U)PBE0/6-311+G(d,p)/Def2-TZVP+ECP level of theory. (SMD = toluene)/CCSD(T)/6-311++G(d,p)/Def2-TZVP+ECP single point corrections are given in parentheses. All energies are in kcal/mol.

Table 4. Distortion-Interaction Analysis to the Au-Catalyzed BC<sup>c</sup>

Reaction	$E_{dist}(comp)$	$E_{int}(comp)$	$E_{dist}(TS)$	$E_{int}(TS)$	$\Delta E_{int}^a$	$\Delta\Delta E^{\ddagger b}$
	4.5 (3.6)	-33.9 (-34.1)	34.0 (31.5)	-48.6 (-47.3)	-14.7 (-13.2)	16.4 (13.4)
	3.2	-35.3	34.4	-52.8	-17.5	18.2
	2.9	-39.9	33.0	-59.1	-19.2	16.7
	3.1	-36.6	25.8	-53.2	-16.6	15.5
	4.8	-40.5	26.4	-53.7	-13.2	24.8

<sup>a</sup>Between TS and reactant complex (catalyzed reaction). <sup>b</sup>Between noncatalyzed and catalyzed reactions. <sup>c</sup>(IEFPCM = toluene)/(U)PBE0/6-311+G(d,p)/Def2-TZVP+ECP level of theory. (SMD = toluene)/CCSD(T)/6-311++G(d,p)/Def2-TZVP+ECP single point corrections in parentheses. Energies in kcal/mol.

noninteracting enediyne/catalyst geometries than the reacting Au/ $\pi$ -complex. Such distortion raises the total energy by 31.5 kcal/mol, a few kcal/mol higher than the barrier for the noncatalyzed Bergman cyclization. However, the interaction energy between catalyst and the substrate increases dramatically relative to that in the Au-substrate complex ( $-34 \rightarrow -46$  kcal/mol!). Thus, the  $\sim 13$  kcal/mol difference between the activation barriers of the thermal and Au-catalyzed BC mostly stems from the additional  $\sim 12$  kcal/mol of substrate/catalyst interaction in the TS.<sup>32</sup>

We attribute such enormous TS stabilization to the multiple roles of Au-catalyst in the TS discussed above: (a) stabilization of the negative charge at C<sub>2</sub> through charge transfer/C–Au bond formation, (b) stabilization of the positive charge through double hyperconjugation, and (c) ensuring favorable symmetry for the bond-forming overlap between the in-plane  $\pi$ -orbitals.

Interestingly, distortion of the catalyst, although minor relative to the distortion of the substrate, also increases in the TS (1.3 kcal/mol in the reactant complex vs 4 kcal/mol in the TS). This process involves lengthening of the Au–P bond due to the increased donation to the  $\sigma_{Au-P}^*$  orbital. Again, this is a reflection of increased donation from the substrate to the catalyst as the reaction progresses.

**Effect of Catalyst.** We have extended the distortion–interaction analysis to other Au(I)-derived species, that is, the AuNHC complex and Au(I) chloride (Table 3). The barrier lowering effect of these catalysts (14.5 and 10.6 kcal/mol relative to the noncatalyzed BC) is lower than the effect of [AuPMe<sub>3</sub>]<sup>+</sup>. Interestingly, AuCl is the least effective catalyst despite making the strongest complex with the enediyne substrate. Distortion–interaction analysis reveals the origin of these differences in the catalytic activity by illustrating that the

change is mostly derived from the difference in the catalyst/substrate interaction energies ( $R^2 = 0.86$ , see the Supporting Information for more information).

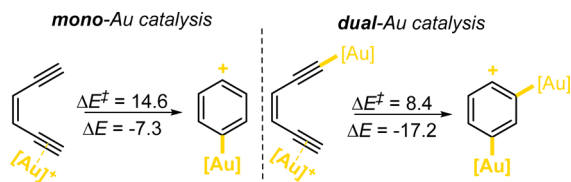
The connection between the catalytic ability and  $\Delta E_{\text{int}}$  values offers a clear guideline for the future experimental design of metal-catalyzed cycloaromatization processes.

**Effect of Substrate.** Expansion of this analysis shows that the catalyst–substrate interaction energies are similarly amplified for the cyclization of other enediyne substrates (Table 4). The data illustrate that the TS-stabilizing interactions can be combined with other factors such as ground-state destabilization. Indeed, the strain effects, known to decrease the activation barriers for noncatalyzed BC, provide a similar decrease for the Au-catalyzed version (31.0  $\rightarrow$  27.6  $\rightarrow$  21.6 kcal/mol (thermal) vs 14.6  $\rightarrow$  10.9  $\rightarrow$  6.1 (Au-catalyzed) for substrates 1  $\rightarrow$  3  $\rightarrow$  4<sup>33</sup>). In other words, constraining of the enediyne moiety within a 10-membered ring has a 3–4 kcal/mol effect at both catalyzed and noncatalyzed processes, whereas adding additional unsaturation in this cycle decreases both barriers by the total of 8–9 kcal/mol. Remarkably, the difference in the barriers of catalyzed and noncatalyzed reactions remains on the order of 15–18 kcal/mol, close to the increase in the substrate/catalyst interaction energies in the TS (15–19 kcal/mol). Other factors such as flexibility of cyclic substrates and additional TS stabilization caused by vicinal hyperconjugation have non-negligible but minor effects (see the Supporting Information).

**Comparison of  $\pi$ - and  $\sigma,\pi$ - (“Dual”) Au-Catalysis of Bergman Cyclization.** Finally, it was interesting to compare the energetics for the mono- and dual Au-catalysis of the Bergman cyclization at the same level of theory and within the same conceptual framework. The comparison illustrates the effect of Au-catalyst  $\pi$ -coordination on the reactivity of an enediyne substrate with a  $\sigma$ -donor substituent at the remote alkyne terminus.

Switching to the dual catalysis leads to additional acceleration of the cycloaromatization step and renders it even more exergonic (Scheme 10). This finding agrees very well with the

**Scheme 10. Activation and Reaction Energies for the Mono and Dual Au-Catalysis of the Bergman Cyclization at the (IEFPCM = toluene)/(U)PBE0/6-311+G(d,p)/Def2-TZVP +ECP Level<sup>a</sup>**



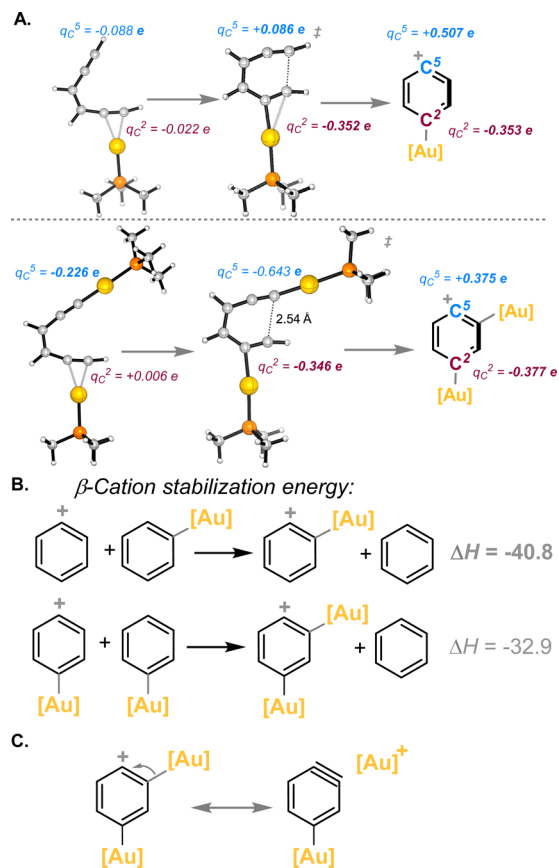
<sup>a</sup>Energies are in kcal/mol.

high efficiency of such transformations documented in the experimental and computational work of Hashmi and co-workers.<sup>18,34</sup> The 6.2 kcal/mol decrease in the activation barrier for the dual-Au system in comparison to the mono-Au case is especially impressive considering that, at the same PBE0/6-311+G(d,p) level of theory, introduction of Au at the terminal alkyne carbon as a  $\sigma$ -substituent has a decelerating effect in comparison to the Bergman cyclization of the parent hydrocarbon ( $\Delta E^\ddagger$  of 32.2 vs 31.0 kcal/mol).

Application of the distortion–interaction analysis shows that, although the catalyst–substrate interaction energies are large for both the prereaction complex and the TS for the dual catalysis system (Table 4), the gain in the stabilizing substrate/catalyst interaction in the TS is slightly decreased in comparison to the mono-Au catalysis mode (13.2 vs 14.7 kcal/mol, respectively). Hence, the accelerating effect of substrate/catalyst coordination is weakened for the dual catalysis mode. However, the difference is compensated by the much lower penalty of distortion from the reactant complex to the TS geometry for the dual catalysis (–5.6 kcal/mol) in comparison to this penalty for the mono-Au catalysis (+3.0 kcal/mol). The large decrease in the cost of distortion is the source of additional acceleration provided by the dual Au catalysis. Scheme 11 illustrates that the *ortho*-Au group significantly decreases positive charge at C<sub>5</sub> of the product and leads to very interesting electron density redistribution in the TS.<sup>35</sup>

**From Interrupted to Aborted Reactions.** The parent BC is an endothermic process with a significant barrier ( $\Delta E(\Delta H)_{\text{rxn}}$

**Scheme 11. (A) Natural Charges for the Mono and Dual Au-Catalysis of the Bergman Cyclization; and (B) Top, the Large Stabilization Energy Caused by [Au] at a  $\beta$ -Position Can Be Associated with the Delocalization of Electronic Density from the C–Au Bond to the Cationic Center at C<sub>5</sub>; Bottom, the Presence of a  $\delta$ -Donor Decreases the Stabilizing Role of the  $\beta$ - $\sigma_{\text{Au-C}}$  Donor in the Product of Dual Au-Catalyzed BC (Also Compare with Scheme 7); and (C) Resonance Structures of Product from Dual-Au Catalysis<sup>a</sup>**



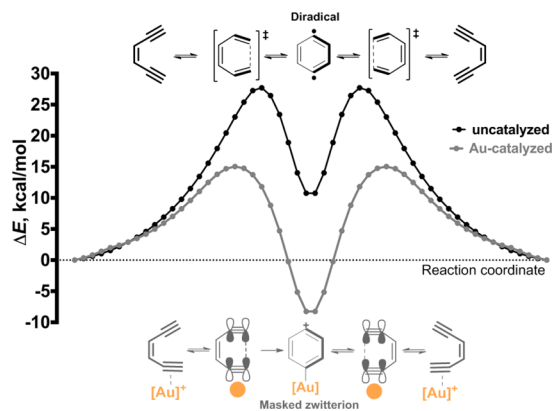
<sup>a</sup>Charges (e) and energies (kcal/mol) at (IEFPCM = toluene)/(U)PBE0/6-311+G(d,p)/Def2-TZVP+ECP level of theory.



$= 7.8(8.5) \pm 1.0$  kcal/mol;  $\Delta E^\ddagger(\Delta H^\ddagger) = 30.1(28.2) \pm 0.5$  kcal/mol).<sup>36</sup> BC can be considered an interrupted pericyclic reaction where aromatic stabilization imposed by the “bystander” out-of-plane aromatic system converts the Cope TS into an energy minimum at the potential energy surface.<sup>37,38</sup> As a result of this stabilization, the cyclic structure can be captured. However, because the equilibrium between cyclic and acyclic structures is heavily shifted to the acyclic reactants, this capture is only efficient if the trapping step is sufficiently fast. If the cyclic diradical intermediate is not trapped, the cycloaromatization process is unproductive; the intermediate either undergoes *retro*-Bergman ring opening back to the reactant or gives the acyclic product of the formal Cope rearrangement. Although the transient nature of the cyclic intermediate is beneficial for the biological role of enediynes as nature’s warheads<sup>39</sup> activated on demand, it more often imposes limitations on the applications of enediynes for the preparation of cyclic structures and occasionally renders the trapping step to be the rate-limiting part of the overall transformation.<sup>40</sup>

Our computations illustrate that the situation changes dramatically and the cyclization becomes  $\sim 7$  kcal/mol exergonic upon coordination of Au-species to one of the triple bonds (Scheme 12). The exergonicity of the cyclization step

**Scheme 12. Potential Energy Surface (PES) for Noncatalyzed (Black) and Au-Catalyzed (Gray) BCs at the (IEFPCM = toluene)/(U)PBE0/6-311+G(d,p)/Def2-TZVP +ECP Level of Theory**



converts BC from an interrupted to an aborted pericyclic reaction (vide infra) and drastically changes the importance of the trapping step for the cyclization efficiency.

Aborted pericyclic reactions are exotic processes where the cyclic TS-like structure corresponds to the global energy minimum, and thus is favored by the equilibrium relative to the acyclic reactants (Scheme 1B).<sup>41</sup> We have shown recently the first example of such behavior in anionic 2,3-sigmatropic shifts (Wittig rearrangements), which can be aborted to become 5-endo cyclizations. We have also shown how a judicious combination of stereoelectronic constraints with organometallic catalysis can convert neutral 3,3-shifts into their interrupted versions.<sup>42</sup> However, the Au-catalyzed BC is the first example of an aborted Cope rearrangement.

## CONCLUSIONS

The chameleonic reactivity of *p*-benzyne spans the continuum between diradical and zwitterionic extremes and reflects the diradical/zwitterion duality, one of the most fundamental

dichotomies in chemistry that manifests itself every time a chemical bond is broken. The present work reveals that the diradical/zwitterion duality exhibits itself in a new role as one of the sources of the catalytic power of Au(I) catalyst in promoting the Bergman cyclization.

Our computations, for the first time, uncover the magnitude of the catalytic effect ( $\sim 16$  kcal/mol barrier decrease with potential for 100 billion-fold acceleration). Furthermore, Au(I)-catalyzed BC is the first example of a Cope rearrangement aborted by the catalyst–substrate interactions. The effect of Au-coordination on the potential energy profile of the archetypal cycloaromatization process reveals stereoelectronic effects associated with the observed changes in reactivity. The Au-catalyst takes multiple roles in this process: from the stereoelectronic support via LUMO umpolung to zwitterionic assistance in stabilization of both negative and positive charges.

Switching from the mono ( $\pi$ -type) to the dual ( $\sigma,\pi$ -type) Au catalysis preserves most of the increase in the stabilizing catalyst–substrate interaction but also significantly decreases the cost of substrate distortion for reaching the TS geometry.

Crossing the diradical/zwitterion threshold allowed the substrate to receive increased stabilization in the TS. We were able to quantify the extent of this stabilization by a new application of distortion–interaction analysis for dissection of electronic and structural consequences of substrate/catalyst interactions. Although this theoretical approach has been, so far, generally applied to bimolecular reactions, we believe the application of the distortion–interaction analysis for homogeneous catalysis highlighted in this work will provide a powerful tool that can be used for a multitude of reactions.

## COMPUTATIONAL METHODS

For the full details for the search of optimal computational methodologies, see the Supporting Information. Unless otherwise noted, we used PBE0, a functional that is known to provide sufficiently accurate description of gold complexes.<sup>43</sup> The 6-311+G(d,p) basis set was employed for C, P, N and H, while Def2-TZVP was used for Au (including effective core potential (ECP)) and Cl; IEFPCM solvation model was adopted to simulate toluene. For the noncatalyzed reactions, we adopted an open-shell, broken-spin symmetry approach. (SMD = toluene)/CCSD(T)/6-311++G(d,p)/Def2-TZVP+ECP single-point corrections were used for the distortion–interaction analysis. Frequency calculations were carried for all structures to confirm them as either a minimum or a TS. Electronic structures and properties were analyzed by the Natural Bond Orbitals (NBO) method at the PBE0 level of theory. Relaxed scans were performed with NBO analysis at each of its steps to track interactions and charges. All calculations were performed with Gaussian 09<sup>44</sup> with the integrated NBO 3.1.<sup>45</sup>

## ASSOCIATED CONTENT

### Supporting Information

The Supporting Information is available free of charge on the ACS Publications website at DOI: 10.1021/jacs.6b11054.

Computational details, functional screening methodologies, NBO scans, and geometries and energies of all reactants, products, complexes, and transition states (PDF)

## AUTHOR INFORMATION

### Corresponding Author

\*alabugin@chem.fsu.edu

### ORCID

Gabriel dos Passos Gomes: 0000-0002-8235-5969

Igor V. Alabugin: 0000-0001-9289-3819

## Notes

The authors declare no competing financial interest.

## ACKNOWLEDGMENTS

This study was supported by the National Science Foundation (Grant CHE-1465142). We are grateful to NSF XSEDE (TG-CHE160006) and RCC FSU for computational resources. G.d.P.G. is grateful to IBM for the 2016 IBM Ph.D. Scholarship.

## REFERENCES

- (1) Gilmore, K.; Mohamed, R. K.; Alabugin, I. V. *WIREs Comput. Mol. Sci.* **2016**, *6*, 487.
- (2) Greer, E. M.; Cosgriff, C. V. *Annu. Rep. Prog. Chem., Sect. B: Org. Chem.* **2013**, *109*, 328.
- (3) For selected examples of cycloaromatization reactions, see: (a) Prall, M.; Wittkopp, A.; Schreiner, P. R. *J. Phys. Chem. A* **2001**, *105*, 9265. (b) Roth, W. R.; Hopf, H.; Horn, C. *Chem. Ber.* **1994**, *127*, 1765. (c) Vavilala, C.; Byrne, N.; Kraml, C. M.; Ho, D. M.; Pascal, R. A. *J. Am. Chem. Soc.* **2008**, *130*, 13549. (d) Engels, B.; Lennartz, C.; Hanrath, M.; Schmittel, M.; Strittmatter, M. *Angew. Chem., Int. Ed.* **1998**, *37*, 1960. (e) Schmittel, M.; Kiau, S.; Siebert, T.; Strittmatter, M. *Tetrahedron Lett.* **1996**, *37*, 7691. (f) Schmittel, M.; Keller, M.; Kiau, S.; Strittmatter, M. *Chem. - Eur. J.* **1997**, *3*, 807. (g) Schmittel, M.; Strittmatter, M.; Kiau, S. *Tetrahedron Lett.* **1995**, *36*, 4975. (h) Reference 10.
- (4) Mohamed, R. K.; Peterson, P. W.; Alabugin, I. V. *Chem. Rev.* **2013**, *113*, 7089.
- (5) Woodward, R. B.; Hoffmann, R. *The Conservation of Orbital Symmetry*; Verlag Chemie: Weinheim, 1970.
- (6) Abe, M. *Chem. Rev.* **2013**, *113*, 7011.
- (7) Grissom, J. W.; Gunawardena, G. U.; Klingberg, D.; Huang, D. *Tetrahedron* **1996**, *52*, 6453.
- (8) Galm, U.; Hager, M. H.; Van Lanen, S. G.; Ju, J.; Thorson, J. S.; Shen, B. *Chem. Rev.* **2005**, *105*, 739.
- (9) (a) Johnson, J. P.; Bringley, D. A.; Wilson, E. E.; Lewis, K. D.; Beck, L. W.; Matzger, A. J. *J. Am. Chem. Soc.* **2003**, *125*, 14708. (b) Smith, D. W.; Shah, H. V.; Perera, K. P. U.; Perpall, M. W.; Babb, D. A.; Martin, S. J. *Adv. Funct. Mater.* **2007**, *17*, 1237.
- (10) (a) Jones, R. R.; Bergman, R. G. *J. Am. Chem. Soc.* **1972**, *94*, 660. (b) Bergman, R. G. *Acc. Chem. Res.* **1973**, *6*, 25.
- (11) Kraka, E.; Cremer, D. *WIREs Comput. Mol. Sci.* **2014**, *4*, 285.
- (12) (a) Perrin, C. L.; Reyes-Rodríguez, G. J. *J. Phys. Org. Chem.* **2013**, *26*, 206. (b) Peterson, P. W.; Mohamed, R. K.; Alabugin, I. V. *Eur. J. Org. Chem.* **2013**, *2013*, 2505.
- (13) Perrin, C. L.; Rodgers, B. L.; O'Connor, J. M. *J. Am. Chem. Soc.* **2007**, *129*, 4795.
- (14) (a) Nguyen, Q. N. N.; Tantillo, D. J. *J. Org. Chem.* **2016**, *81*, 5295. (b) Gonçalves, T. P.; Mohamed, M.; Whitby, R. J.; Sneddon, H. F.; Harrowven, D. C. *Angew. Chem.* **2015**, *127*, 4614.
- (15) For the first gold-catalyzed arene synthesis, see: Hashmi, A. S. K.; Frost, T. M.; Bats, J. W. *J. Am. Chem. Soc.* **2000**, *122*, 11553.
- (16) For a formal Myers–Saito cyclization, see: Zhao, J.; Hughes, C. O.; Toste, F. D. *J. Am. Chem. Soc.* **2006**, *128*, 7436.
- (17) (a) Hashmi, A. S. K. *Angew. Chem., Int. Ed.* **2010**, *49*, 5232–524. (b) de Oteyza, D. G.; Pérez Paz, A.; Chen, Y.-C.; Pedramrazi, Z.; Riss, A.; Wickenburg, S.; Tsai, H.-Z.; Fischer, F. R.; Crommie, M. F.; Rubio, A. *J. Am. Chem. Soc.* **2016**, *138*, 10963. (c) Wang, Q.; Aparaj, S.; Akhmedov, N. G.; Petersen, J. L.; Shi, X. *Org. Lett.* **2012**, *14*, 1334. (d) Chen, Y.; Chen, M.; Liu, Y. *Angew. Chem., Int. Ed.* **2012**, *51*, 6493. (e) Hou, W.; Zhang, Z.; Kong, F.; Wang, S.; Wang, H.; Yao, Z.-J. *Chem. Commun.* **2013**, *49*, 695. (f) Hashmi, A. S. K.; Braun, I.; Nösel, P.; Schädlich, J.; Wietek, M.; Rudolph, M.; Rominger, F. *Angew. Chem., Int. Ed.* **2012**, *51*, 4456. (g) Hashmi, A. S. K.; Frost, T. M.; Bats, J. W. *J. Am. Chem. Soc.* **2000**, *122*, 11553.
- (18) For a recent review, see: Pflästerer, D.; Hashmi, A. S. K. *Chem. Soc. Rev.* **2016**, *45*, 1331.
- (19) (a) Naoe, S.; Suzuki, Y.; Hirano, K.; Inaba, Y.; Oishi, S.; Fujii, N.; Ohno, H. *J. Org. Chem.* **2012**, *77*, 4907. (b) Byers, P. M.; Rashid, J. I.; Mohamed, R. K.; Alabugin, I. V. *Org. Lett.* **2014**, *14*, 6032.
- (20) Ye, L.; Wang, Y.; Aue, D. H.; Zhang, L. *J. Am. Chem. Soc.* **2012**, *134*, 31.
- (21) (a) Hong, Y. J.; Tantillo, D. J. *Nat. Chem.* **2014**, *6*, 104. (b) Hansmann, M. M.; Rudolph, M.; Rominger, F.; Hashmi, A. S. K. *Angew. Chem., Int. Ed.* **2013**, *52*, 2593.
- (22) (a) Hashmi, A. S. K. *Acc. Chem. Res.* **2014**, *47*, 864. (b) Hashmi, A. S. K.; Braun, I.; Rudolph, M.; Rominger, F. *Organometallics* **2012**, *31*, 644. (c) For a detailed analysis on stepwise catalyst transfer, see: Larsen, M. H.; Houk, K. N.; Hashmi, A. S. K. *J. Am. Chem. Soc.* **2015**, *137*, 10668.
- (23) (a) Alabugin, I. V.; Gilmore, K.; Manoharan, M. *J. Am. Chem. Soc.* **2011**, *133*, 12608. (b) Gilmore, K.; Alabugin, I. V. *Chem. Rev.* **2011**, *111*, 6513.
- (24) Alabugin, I. V.; Manoharan, M. *J. Phys. Chem. A* **2003**, *107*, 3363.
- (25) Alabugin, I. V.; Gilmore, K. *Chem. Commun.* **2013**, *49*, 11246. See also ref 1..
- (26) (a) For an example of an intermolecular Au-catalyzed thermal [2+2] alkyne-alkene cycloaddition, see: López-Carrillo, V.; Echavarren, A. M. *J. Am. Chem. Soc.* **2010**, *132*, 929. (b) For selected intermolecular versions of this process, see: Obradors, C.; Leboeuf, D.; Aydin, J.; Echavarren, A. M. *Org. Lett.* **2013**, *15*, 1576. (c) Homs, A.; Obradors, C.; Leboeuf, D.; Echavarren, A. M. *Adv. Synth. Catal.* **2014**, *356*, 221. (d) Ranieri, B.; Obradors, C.; Mato, M.; Echavarren, A. M. *Org. Lett.* **2016**, *18*, 1614.
- (27) NBO analysis transforms the canonical delocalized molecular orbitals from DFT calculations into localized orbitals that are closely tied to the chemical bonding concepts. Each of the localized NBO sets is complete and orthonormal. The filled NBOs describe the hypothetical, strictly localized Lewis structure. The interactions between filled and antibonding orbitals represent the deviation from the Lewis structure and can be used to measure delocalization. For example, delocalizing interaction can be treated via the second-order perturbation energy approach as  $E(2) = \frac{n_i F_{ij}^2}{\Delta E}$ , where  $n_i$  is the population of a donor orbital,  $F_{ij}$  is the Fock matrix element for the interacting orbitals  $i$  and  $j$ , and  $\Delta E$  is the energy gap between these orbitals.
- (28) Logan, C. F.; Chen, P. *J. Am. Chem. Soc.* **1996**, *118*, 2113.
- (29) (a) Mohamed, R.; Mondal, S.; Gold, B.; Evoniuk, C. J.; Banerjee, T.; Hanson, K.; Alabugin, I. V. *J. Am. Chem. Soc.* **2015**, *137*, 6335. (b) Mondal, S.; Gold, B.; Mohamed, R. K.; Alabugin, I. V. *Chem. - Eur. J.* **2014**, *20*, 8664.
- (30) (a) Alabugin, I. V.; Manoharan, M. *J. Org. Chem.* **2004**, *69*, 9011. (b) Alabugin, I. V. *Stereoelectronic Effects: A Bridge Between Structure and Reactivity*; John Wiley & Sons, Ltd.: Chichester, UK, 2016.
- (31) (a) Ess, D. H.; Houk, K. N. *J. Am. Chem. Soc.* **2007**, *129*, 10646. (b) Hayden, A. E.; Houk, K. N. *J. Am. Chem. Soc.* **2009**, *131*, 4084. (c) Jones, G. O.; Houk, K. N. *J. Org. Chem.* **2008**, *73*, 1333. (d) Ess, D. H.; Jones, G. O.; Houk, K. N. *Org. Lett.* **2008**, *10*, 1633. (e) Ess, D. H.; Houk, K. N. *J. Am. Chem. Soc.* **2008**, *130*, 10187. (f) Xu, L.; Doubleday, C. E.; Houk, K. N. *Angew. Chem., Int. Ed.* **2009**, *48*, 2746. (g) Lan, Y.; Houk, K. N. *J. Am. Chem. Soc.* **2010**, *132*, 17921. (h) Krenske, E. H.; Houk, K. N.; Holmes, A. B.; Thompson, J. *Tetrahedron Lett.* **2011**, *52*, 2181. (i) Schoenebeck, F.; Ess, D. H.; Jones, G. O.; Houk, K. N. *J. Am. Chem. Soc.* **2009**, *131*, 8121. (j) Krenske, E. H.; Pryor, W. A.; Houk, K. N. *J. Org. Chem.* **2009**, *74*, 5356. (k) Osuna, S.; Houk, K. N. *Chem. - Eur. J.* **2009**, *15*, 13219. (l) van Zeist, W.-J.; Bickelhaupt, F. M. *Org. Biomol. Chem.* **2010**, *8*, 3118. For applications to metal-catalyzed reactions, see: (m) Wolf, L. M.; Thiel, W. *J. Org. Chem.* **2014**, *79*, 12136. (n) Xu, H.; Muto, K.; Yamaguchi, J.; Zhao, C.; Itami, K.; Musaev, D. G. *J. Am. Chem. Soc.* **2014**, *136*, 14834.

(32) For additional examples of polar catalyst interacting with and changing the nature of nonpolar pericyclic transition states, see: Tantillo, D. *Acc. Chem. Res.* **2016**, *49*, 741.

(33) This molecule has been shown to undergo direct and retro-Bergman cyclization by atomic manipulation: Schuler, B.; Fatayer, S.; Mohn, F.; Moll, N.; Pavliček, N.; Meyer, G.; Peña, D.; Gross, L. *Nat. Chem.* **2016**, *8*, 220.

(34) For a deeper exploration of the thermodynamics of the dual-Au catalysis on the Bergman cyclization, see: Vilhelmsen, M. H.; Hashmi, A. S. K. *Chem. - Eur. J.* **2014**, *20*, 1901 The activation energies in the work of Vilhelmsen et al. agree with our data.

(35) An intriguing possible explanation to the decreased distortion penalty is an increase in hyperconjugative interaction between the donor  $\sigma_{C6-Au}$  bond and the breaking in-plane  $\pi_{C5C6}$  bond as the latter is being transformed into the cationic center at C5. A polarity-inverted version of such hyperconjugative assistance to bond-breaking is used for facilitating cycloaddition reactions: Gold, B.; Batsomboon, P.; Dudley, G. B.; Alabugin, I. V. *J. Org. Chem.* **2014**, *79*, 6221. Gold, B.; Dudley, G. B.; Alabugin, I. V. *J. Am. Chem. Soc.* **2013**, *135*, 1558. Gold, B.; Shevchenko, N.; Bonus, N.; Dudley, G. B.; Alabugin, I. V. *J. Org. Chem.* **2012**, *77*, 75. Gold, B.; Aronoff, M. A.; Raines, R. T. *Org. Lett.* **2016**, *18*, 4466. Aronoff, M. A.; Gold, B.; Raines, R. T. *Tetrahedron Lett.* **2016**, *57*, 2347.

(36) Roth, W. R.; Hopf, H.; Horn, C. *Chem. Ber.* **1994**, *127*, 1765.

(37) Navarro-Vázquez, A.; Prall, M.; Schreiner, P. R. *Org. Lett.* **2004**, *6*, 2981. For reviews, see: Graulich, N.; Hopf, H.; Schreiner, P. R. *Chem. Soc. Rev.* **2010**, *39*, 1503. Graulich, N. *WIREs Comput. Mol. Sci.* **2011**, *1*, 172.

(38) For other selected structural perturbations and substituent effects that can completely or partially uncouple bond-breaking and bond-making in the Cope rearrangement, see: Carpenter, B. K. *Tetrahedron* **1978**, *34*, 1877. Doering, W. von E.; Birladeanu, L.; Sarma, K.; Blaschke, G.; Scheidemantel, U.; Boese, R.; Benet-Bucholz, J.; Klärner, F.-G.; Gehrke, J. – S.; Zinny, B. U.; Sustmann, R.; Korth, H.-G. *J. Am. Chem. Soc.* **2000**, *122*, 193. Roth, W. R.; Lennartz, H.-W.; Doering, W. v. E.; Birladeanu, L.; Guyton, C. A.; Kitagawa, T. *J. Am. Chem. Soc.* **1990**, *112*, 1722. Jiao, H.; Nagelkerke, R.; Kurtz, H. A.; Williams, R. V.; Borden, W. T.; Schleyer, P. v. R. *J. Am. Chem. Soc.* **1997**, *119*, 5921. Roth, W. R.; Gleiter, R.; Paschmann, V.; Hackler, U. E.; Fritzsche, G.; Lange, H. *Eur. J. Org. Chem.* **1998**, *2*, 961. Hrovat, D. A.; Beno, B. R.; Lange, H.; Yoo, H. – Y.; Houk, K. N.; Borden, W. T. *J. Am. Chem. Soc.* **1999**, *121*, 10529. Hrovat, D. A.; Chen, J.; Houk, K. N.; Borden, W. T. *J. Am. Chem. Soc.* **2000**, *122*, 7456. Black, K. A.; Wilsey, S.; Houk, K. N. *J. Am. Chem. Soc.* **2003**, *125*, 6715. Pal, R.; Clark, R. J.; Manoharan, M.; Alabugin, I. V. *J. Org. Chem.* **2010**, *75*, 8689. Borden, W. T. *J. Org. Chem.* **2011**, *76*, 2943.

(39) (a) Nicolaou, K. C.; Smith, A. L. *Acc. Chem. Res.* **1992**, *25*, 497.

(b) Gleiter, R.; Kratz, D. *Angew. Chem., Int. Ed. Engl.* **1993**, *32*, 842.

(40) (a) Zeidan, T. A.; Manoharan, M.; Alabugin, I. V. *J. Org. Chem.* **2006**, *71*, 954. (b) Baroudi, A.; Mauldin, J.; Alabugin, I. V. *J. Am. Chem. Soc.* **2010**, *132*, 967.

(41) Gilmore, K.; Manoharan, M.; Wu, J. I.-C.; Schleyer, P. V. R.; Alabugin, I. V. *J. Am. Chem. Soc.* **2012**, *134*, 10584.

(42) Vidhani, D. V.; Krafft, M. E.; Alabugin, I. V. *J. Am. Chem. Soc.* **2016**, *138*, 2769.

(43) Kang, R.; Chen, H.; Shaik, S.; Yao, J. *J. Chem. Theory Comput.* **2011**, *7*, 4002.

(44) Frisch, M. J.; et al. *Gaussian 09*, revision D.01; Gaussian, Inc.: Wallingford, CT, 2009. The complete reference can be found in the [Supporting Information](#).

(45) Weinhold, F.; Landis, C. R.; Glendening, E. D. *Int. Rev. Phys. Chem.* **2016**, *35*, 1. Reed, A. E.; Weinhold, F. *J. Chem. Phys.* **1985**, *83*, 1736. Reed, A. E.; Weinhold, F. *Isr. J. Chem.* **1991**, *31*, 277. Reed, A. E.; Curtiss, L. A.; Weinhold, F. *Chem. Rev.* **1988**, *88*, 899. Weinhold, F. In *Encyclopedia of Computational Chemistry*; Schleyer, P. v. R., Ed.; Wiley: New York, 1998; Vol. 3, p 1792.